J. Chem. Eng. Data 1988, 33, 310-313

Activity Coefficients in Thiophene–Butanol Systems near the Freezing Point of Thiophene

Fernando Aguirre-Ode* and Joel Koo

Departamento de Quîmica, Facultad de Ciencia, Universidad Têcnica Federico Santa María, Valparaíso, Chile

Activity coefficients of four butanols and thiophene are determined by measuring freezing point lowering of solutions of alcohols in thiophene. Fits to van Laar, Wilson, and some continuous association models showed that the latter models work much better in all cases, considering monomers as the minor species in each alcohol. The magnitudes of the association equilibrium constants in the low-concentration range are much lower than those calculated on the basis of properties of pure alcohols with athermal models of continuous association. Besides, ideal associated solution models fit much better than athermal associated solution models.

Introduction

Measurements of freezing point depressions of a solvent have been widely used in the determination of molecular weights and activity coefficients in the region of high dilution of the solute. Recently, activity coefficients of cyclohexane–alcohol systems near the freezing point of cyclohexane have been calculated (*1*) showing a better fit to continuous association models than to some traditional solutions models.

A similar calculation is presented herein, involving thiophene as the solvent and the four butanols as solutes. Experimental activity coefficients in the region of high dilution of the alcohol are presented. A fit to six different models shows analogous trends, except for the fact that, in this case, monomers appear to be the minor species in all cases. When cyclohexane was the solvent, dimers were the smallest species in most alcohols, *tert*-butyl alcohol being the solute with tetramers as the predominating species.

Experimental Section

The butanols, thiophene, and chlorobenzene were analytical grade reagents from Merck with certified minimum purities of 99.0%. For this reason, they were redistilled with magnesium in a high-efficiency packed column. A heart cut was collected by discarding the first 20% distillate and the last 25% residue. The physical properties showed good agreement with the values from literature (*2*, *3*) and they are detailed in Table I. A chromatographic analysis of chlorobenzene indicated the presence of 0.006% of benzene by volume.

The experimental procedure was basically that described by Gillespie et al. (*4*). Figure 1 shows the schematic arrangement of the different elements of work. The bath B contained 6.5 L of ethyl alcohol, externally protected by a commercial thermal insulator A. Stirrer D helped to maintain homogeneity of the temperature through the bath, regulated by cooler C, heater H, and thermal sensor S of the cooling system Flexi-Cool, FTS System Inc., Model FC-20-60-P4. The helical stirrer within the container G was activated by an electromagnetic coil E refrigerated by a water jacket and controlled by a voltage regulator connected and disconnected intermittently through a small copper sheet in a rotating disk.

A Thermo-Schneider thermometer, T, for the range −30 to −62 °C, was used to determine the temperature versus time cooling curves for the solvent alone and for different concentrations of each of the solutes. The points −38.30 and −45,21 °C were calibrated against the freezing points of pure thiophene and pure chlorobenzene, respectively. A magnifying glass M allowed to read with a precision of 0.01 °C.

Table I. Observed Physical Properties of Reagents

reagent	refractive index[a]	normal bp, °C
thiophene	1.5287	84.11
1-butanol	1.3993	117.70
2-butanol	1.3971	99.47
isobutyl alcohol	1.3958	107.82
tert-butyl alcohol	1.3824[a]	82.40
chlorobenzene	1.5246	131.80

[a] Measured at 25.00 °C, except *tert*-butyl alcohol whose index was measured at 30.00 °C.

Samples were prepared by a continuous dilution procedure. Mole fractions were determined by weighing solvent and solute.

The freezing point depression, θ_m, directly obtained from the experimental measurements, was corrected for the supercooling effect in the manner suggested by Gillespie et al. (*4*)

$$\hat{\theta} = \theta_m \left(1 - \frac{c_p}{\lambda_1} S\right) \qquad (1)$$

in which c_p is the heat capacity of liquid thiophene, λ_1, is the heat of fusion of the same solvent, $S = T - T_s$ is the extent of the supercooling, T is the freezing point, and T_s is the lowest temperature of the supercooled system. Values of $\hat{\theta}$ differ from θ_m by no more than 0.01 on the average.

Calculation of Activity Coefficients from Experimental Data

From the thermodynamic analysis of solid–liquid equilibrium, the following equation is derived

$$\mathrm{d} \ln a_1 = -(\lambda_1/R)\, \mathrm{d}(1/T) \qquad (2)$$

in which a_1 is the activity of the solvent, λ_1 the heat of fusion of the solvent [J/mol], R the gas constant [J/(mol K)], and T the absolute temperature [K].

As the heat of fusion is dependent upon the temperature, a series expansion in terms of the freezing point lowering, θ, allows one to write (*5*) after substitution and integration of eq 2

$$\ln a_1 = -\theta(A + B\theta + \ldots) \qquad (3)$$

in which $A = \lambda_1/RT_0^2$, $B = (A - \Delta c_p/2RT_0)/T_0$, T_0 is the melting point of the solvent [K], and Δc_p is the specific heat capacity difference of liquid and solid thiophene [J/(mol K)].

For thiophene, the following figures were calculated from measured or reference data (*6*, *7*): $\lambda_1 = 5085.6$ J/mol; $\Delta c_p = -18.9$ J/(mol K); $T_0 = 234.85$ K; $A = 0.011090$; $B = 2.6602 \times 10^{-5}$.

B being so small in comparison with A, eq 3 can be linearized keeping only the first term in the series.

For the calculation of activity coefficients it is common practice to use the osmotic coefficient, ϕ, defined in the following manner

$$\phi = (\ln a_1)/\ln x_1 \qquad (4)$$

0021-9568/88/1733-0310$01.50/0

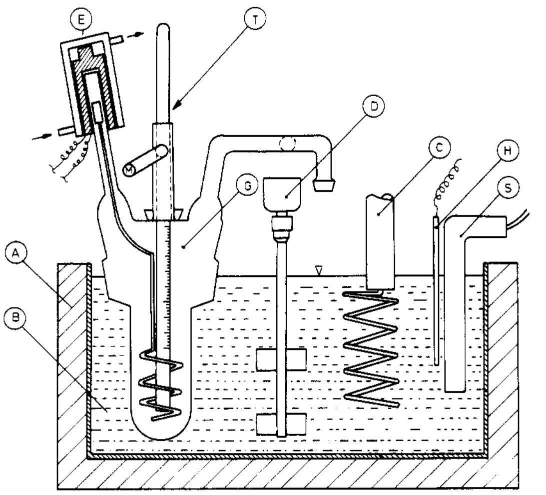

Figure 1. Schematic diagram of the cryoscopic measuring system.

Table II. Parameters and Standard Deviations When Smoothing Data with Eq 8

solute	data point	A_0	A_1	A_2	σ, °C
1-butanol	28	0.015 456 0	1.179 725	−0.252 937 6	0.024
2-butanol	17	0.015 214 4	1.273 065	−0.544 019 6	0.019
isobutyl alcohol	19	0.017 774 0	1.166 510	−0.359 678 8	0.024
tert-butyl alcohol	12	0.014 149 6	1.262 356	0.021 816 5	0.012

It can be shown by a series expansion that the following approximation is valid for low values of x_2, the mole fraction of the solute

$$\phi = -(\ln a_1)/z \tag{5}$$

in which $z = x_2/x_1$, the mole fraction ratio.

On the other hand, it was empirically realized that the ratio $z/(1 - \phi)$ behaved as a parabolic function of z in all cases

$$z/(1 - \phi) = A_0 + A_1z + A_2z^2 \tag{6}$$

in which A_0, A_1, and A_2 are the best parameters from the minimization of the objective function

$$\psi_\theta = \sum_k^N (\theta - \hat{\theta})_k^2 \tag{7}$$

N is the number of experimental data points, $\hat{\theta}$ is the experimental freezing point lowering, and θ is the calculated value

$$\theta = \frac{z[A_0 + (A_1 - 1)z + A_2z^2]}{A[A_0 + A_1z + A_2z^2]} \tag{8}$$

The quality of the smoothing of the experimental data can be appreciated from Table II, in which optimum values of A_0, A_1, and A_2, together with the respective standard deviations of the fits, are shown for each system. Standard deviations are low enough as to support the applicability of the empirical eq 6.

The following step was the calculation of the activity coefficients as a function of the stoichiometric mole fractions, i.e., those which come from considering monomers of alcohol as the solute. The behavior of the osmotic coefficient was such that the quantity $(1 - \phi)$ did approach naturally to zero when extrapolated for $z = 0$, which is an evidence for considering monomers as the minor species at high dilution.

The activity coefficients of the solvent were calculated with the following equation:

$$\hat{\gamma}_1 = \frac{\exp(A\theta z)}{x_1} \tag{9}$$

The activity coefficients of the solute are calculated by using infinitely dilute alcohol as the reference state. From Gibbs–Duhem equation and eq 5

$$\ln \gamma_2 x_1 = -(1 - \phi) - \int_0^z \frac{(1 - \phi)}{z}\, dz \tag{10}$$

is obtained following a treatment analogous to that given by Prigogine and Defay (*8*).

By taking into consideration the form of eq 6, the integration of eq 10 can be done analytically. The following result is obtained

$$\hat{\gamma}_2 = \frac{\eta}{x_1} \exp\left[-\frac{z}{A_0 + A_1z + A_2z^2}\right] \tag{11}$$

in which

$$\eta = [\{1 + 2A_2z/(A_1 + \epsilon)\}/\{1 + 2A_2z/(A_1 - \epsilon)\}]^\epsilon \tag{12}$$

$$\epsilon = \{A_1^2 - 4A_0A_2\}^{1/2} \tag{13}$$

when $A_1^2 > 4A_0A_2$, and

$$\eta = \exp\left[\frac{2}{\epsilon}\left\{\tan^{-1}(A_1/\epsilon) - \tan^{-1}\left(\frac{A_1 + A_2z}{\epsilon}\right)\right\}\right] \tag{14}$$

$$\epsilon = \{4A_0A_2 - A_1^2\}^{1/2} \tag{15}$$

when $A_1^2 < 4A_0A_2$.

Table III gives mole fractions, experimental freezing point lowerings, and activity coefficients calculated in the described manner.

Correlation of Activity Coefficients with Models

In order to appraise the interpretative ability of several simple models with regard to the activity coefficients calculated in the proceeding section, a fit of them had to be made. The same objective function was used in all cases

$$\psi_\gamma = \sum_j^2 \sum_k^N \{1 - (\gamma_j/\hat{\gamma}_j)\}_k^2 \tag{16}$$

and standard deviations were determined according to

$$\sigma = 100\{\psi_\gamma/(N - 1)\}^{1/2} \tag{17}$$

γ_j and $\hat{\gamma}_j$ are respectively calculated from the model and from the experimental data.

The equations for calculating activity coefficients are those of the six models already detailed elsewhere (*1*):

model I: van Laar (*9*)

model II: Wilson (*10*)

model III: ideal associated solution with two equilibrium constants (*11*)

model IV: ideal associated solution with equilibrium constant dependent on the degree of association (*12*)

model V: athermal associated solution with two equilibrium constants (*1*)

model VI: athermal associated solution with only one equilibrium constant, K, and physical interaction contributions (*13*)

In most cases, the computational procedure followed Newton–Raphson method to localize the minimum of the objective

Table III. Mole Fractions, Experimental Freezing Point Lowerings, and Activity Coefficients from Experimental Data

x_2	$\hat{\theta}$, °C	$\hat{\gamma}_1$	$\hat{\gamma}_2$	x_2	$\hat{\theta}$, °C	$\hat{\gamma}_1$	$\hat{\gamma}_2$
Thiophene (1)–1-Butanol (2)							
0.0131	0.69	1.0056	0.3646	0.0374	1.24	1.0243	0.1705
0.0167	0.82	1.0080	0.3111	0.0374	1.25	1.0243	0.1705
0.0167	0.83	1.0080	0.3111	0.0416	1.30	1.0280	0.1564
0.0173	0.81	1.0084	0.3042	0.0416	1.30	1.0280	0.1564
0.0217	0.94	1.0117	0.2584	0.0579	1.59	1.0424	0.1194
0.0217	0.96	1.0117	0.2584	0.0579	1.59	1.0424	0.1194
0.0228	0.98	1.0125	0.2491	0.0815	2.02	1.0649	0.0896
0.0264	1.03	1.0153	0.2234	0.0815	2.03	1.0649	0.0896
0.0264	1.06	1.0153	0.2234	0.1124	2.43	1.0967	0.0680
0.0297	1.15	1.0180	0.2039	0.1124	2.43	1.0967	0.0680
0.0314	1.15	1.0193	0.1956	0.1474	2.87	1.1361	0.0536
0.0314	1.17	1.0193	0.1956	0.1474	2.87	1.1361	0.0536
0.0337	1.20	1.0212	0.1850	0.1746	3.16	1.1697	0.0460
0.0337	1.20	1.0212	0.1850	0.1746	3.17	1.1697	0.0460
Thiophene (1)–2-Butanol (2)							
0.0157	0.79	1.0071	0.3321	0.0617	1.87	1.0436	0.1227
0.0222	0.98	1.0116	0.2636	0.0898	2.37	1.0695	0.0907
0.0222	0.98	1.0116	0.2636	0.0905	2.42	1.0703	0.0900
0.0225	0.98	1.0118	0.2610	0.0905	2.43	1.0703	0.0900
0.0225	0.99	1.0118	0.2610	0.1258	2.98	1.1065	0.0683
0.0285	1.13	1.0162	0.2208	0.1262	2.98	1.1070	0.0681
0.0285	1.14	1.0162	0.2208	0.1262	3.00	1.1070	0.0681
0.0342	1.34	1.0206	0.1930	0.1686	3.48	1.1568	0.0527
0.0397	1.45	1.0250	0.1726				
Thiophene (1)–Isobutyl Alcohol (2)							
0.0094	0.61	1.0031	0.4805	0.0357	1.29	1.0222	0.1950
0.0094	0.62	1.0031	0.4805	0.0383	1.33	1.0244	0.1844
0.0145	0.78	1.0061	0.3728	0.0407	1.39	1.0265	0.1756
0.0145	0.79	1.0061	0.3728	0.0587	1.70	1.0427	0.1298
0.0145	0.79	1.0061	0.3728	0.0597	1.67	1.0436	0.1279
0.0199	0.88	1.0098	0.3017	0.0856	2.05	1.0689	0.0940
0.0199	0.90	1.0098	0.3017	0.0856	2.06	1.0689	0.0940
0.0252	1.05	0.0138	0.2543	0.1247	2.48	1.1114	0.0672
0.0303	1.17	1.0178	0.2218	0.1645	2.76	1.1604	0.0520
0.0303	1.19	1.0178	0.2218				
Thiophene (1)–*tert*-Butyl Alcohol (2)							
0.0081	0.48	1.0027	0.4695	0.0213	0.95	1.0112	0.2574
0.0096	0.56	1.0035	0.4274	0.0250	1.01	1.0139	0.2303
0.0102	0.58	1.0039	0.4127	0.0273	1.11	1.0156	0.2163
0.0132	0.68	1.0057	0.3535	0.0318	1.20	1.0190	0.1936
0.0159	0.77	1.0075	0.3138	0.0363	1.31	1.0226	0.1755
0.0205	0.92	1.0106	0.2649	0.0387	1.39	1.0244	0.1675

Table IV. Parameters and Percentagewise Standard Deviations for Model I (van Laar)

solute	A_{21}	A_{12}	σ
1-butanol	3.181	0.232	7.29
2-butanol	2.995	0.208	6.76
isobutyl alcohol	3.034	0.226	7.41
tert-butyl alcohol	2.326	0.090	1.44

Table V. Parameters[a] and Percentagewise Standard Deviations for Model II (Wilson)

solute	$\lambda_{12} - \lambda_{22}$	$\lambda_{12} - \lambda_{11}$	σ
1-butanol	1827	−50	2.00
2-butanol	1810	−137	2.66
isobutyl alcohol	1777	−29	2.08
tert-butyl alcohol	1911	−396	0.58

[a] $\lambda_{ij} - \lambda_{jj}$ is given in calories/mole.

Table VI. Parameters and Percentagewise Standard Deviations for Model III (Two-Constant Ideal Associated Solution)

solute	K_1	K_2	σ
1-butanol	61.2	106.0	0.33
2-butanol	73.1	90.6	0.33
isobutyl alcohol	47.0	98.4	0.41
tert-butyl alcohol	71.9	101.1	0.30

Table VII. Parameters and Percentagewise Standard Deviations with Model IV (Ideal Associated Solution with Gradually Varying Equilibrium Constant)

solute	K	β	σ
1-butanol	76.7	0.337	0.85
2-butanol	79.1	0.667	0.45
isobutyl alcohol	60.8	0.095	0.63
tert-butyl alcohol	77.9	0.359	0.47

Table VIII. Parameters and Percentagewise Standard Deviations with Model V (Athermal Associated Solution with Two Equilibrium Constants)

solute	K_1	K_2	σ
1-butanol	94.2	122.3	1.56
2-butanol	115.7	106.3	1.26
isobutyl alcohol	83.0	110.4	1.97
tert-butyl alcohol	133.8	111.7	0.38

Table IX. Parameters and Percentagewise Standard Deviations with Model VI (Athermal Associated Solution with Physical Interaction Contributions: $\beta = 0$)

solute	K	χ[a]	σ
1-butanol	113.2	5.42	0.59
2-butanol	108.0	−0.34	1.40
isobutyl alcohol	98.7	9.28	0.43
tert-butyl alcohol	124.2	−17.29	0.04

[a] χ is given in calories/mole.

Table X. Average Percentagewise Deviations

model	deviation
I. van Laar	5.72 ± 2.87
II. Wilson	1.83 ± 0.83
III. ideal associated (K_1, K_2)	0.34 ± 0.05
IV. ideal associated (K, β)	0.60 ± 0.18
V. athermal associated (K_1, K_2)	1.29 ± 0.67
VI. athermal associated (K, χ)	0.62 ± 0.56

Table XI. Comparison of K_2 from Model V with K_A from Nath and Bender (*14*)

solute	K_2	K_A
1-butanol	122.3	1060
2-butanol	106.3	545
isobutyl alcohol	110.4	277
tert-butyl alcohol	111.7	136

function, ψ_γ. In some cases, it had to be replaced or complemented by a sort of trial and error procedure.

Results and Discussion

Tables IV–IX give the respective optimum parameters and percentagewise standard deviations. Table X compares average percentagewise standard deviations of the four butanols for the six models.

Athermal associated solution models III, IV, and VI show better results than the other three models. However, a careful examination of Table IX allows one to see that there is a sort of compensation effect in model VI, arising from the physical interaction parameter, χ, since it shows no rational trend from one alcohol to the other.

Model III is the best one for all alcohols, followed very closely by model IV. Both of them consider ideal associated solutions, i.e., no physical interaction contributions and no Flory's entropy effect. There is appreciable greater deviation in passing from the ideal associated (Tables VI and VII) to the athermal associated solution model (Tables VIII and IX).

In the low concentration region herein examined, chemical equilibrium constants are much lower than those calculated from pure alcohol properties (*14*) (Table XI). More recent information (*15*) about equilibrium constants does not alter significantly the differences. It must be pointed out, however, that these constants are extrapolated from vapor pressure data at temperatures higher than those considered in this work.

Again, as in the case of cyclohexane as the solvent (*1*) the differences may be attributed to an influence of the concentration in the region of high dilution, in spite of the aromaticity of thiophene, which should be considered in some way in the theory of associated solutions.

Glossary

a_1	activity of the solvent
A, B	constants (see eq 3)
A_0, A_1, A_2	constants (see eq 6)
A_{12}, A_{21}	van Laar parameters
c_p	heat capacity
K, K_A, K_1, K_2	chemical equilibrium constants
N	number of experimental data points
R	gas constant
S	extent of supercooling
T	absolute temperature
T_0	melting point of the solvent
T_s	lowest temperature of supercooled solution
x_1, x_2	mole fractions of solvent and solute
z	mole fraction ratio x_2/x_1
β	parameter in ideal associated solution model
γ_1, γ_2	activity coefficients of solvent and solute
Δ	difference
ϵ	see eq 13 and 15
η	see eq 12 and 14
θ	freezing point depression calculated from a model
$\hat{\theta}$	corrected experimental freezing point depression
θ_m	measured experimental freezing point depression
λ_{ij}, Λ_{ij}	Wilson equation parameters
λ_1	heat of fusion of solvent
σ	standard deviation
ϕ	osmotic coefficient
χ	Scatchard–Hildebrand type parameter
ψ_θ, ψ_γ	objective functions

Registry No. Thiophene, 110-02-1; 1-butanol, 71-36-3; 2-butanol, 78-92-2; isobutyl alcohol, 78-83-1; *tert*-butyl alcohol, 75-65-0.

Literature Cited

(1) Aguirre-Ode, F. *J. Chem. Eng. Data* **1987**, *32*, 434.
(2) Timmermans, J. *Physico-Chemical Constants of Pure Organic Compounds*; Elsevier: New York, 1950.
(3) Wilhoit, R. C., Zwolinski, B. J., *J. Phys. Chem. Ref. Data* **1973**, *2*, Suppl. No. 1.
(4) Gillespie, R. J., Hughes, E. D., Ingold, C. K. *J. Chem. Soc.* **1950**, 2472.
(5) Prigogine, I., Defay, R. *Chemical Thermodynamics*; Wiley: New York, 1962; p 359.
(6) Waddington, G., Knowlton, J. *J. Am. Chem. Soc.* **1949**, *71*, 798.
(7) Figuiere, P., Szwarc, H., Masaharu, O., Suga, H. *J. Chem. Thermodyn.* **1985**, *17*, 949.
(8) Prigogine, I., Defay, R. *Chemical Thermodynamics*; Wiley: New York, 1962; p 324.
(9) van Laar, J. J. *Z. Phys. Chem.* **1910**, *72*, 723.
(10) Wilson, G. M. *J. Am. Chem. Soc.* **1984**, *86*, 127.
(11) Aguirre-Ode, F. *Scientia* **1977**, *42*(149), 25.
(12) Aguirre-Ode, F. *Scientia* **1979**, *44*(152), 19.
(13) Aguirre-Ode, F. *Fluid Phase Equilib.* **1986**, *30*, 315.
(14) Nath, A., Bender, E. *Fluid Phase Equilib.* **1981**, *7*, 275.
(15) Hofman, T., Nagata, I. *Fluid Phase Equilib.* **1986**, *25*, 113.

Received for review July 22, 1987. Revised February 16, 1988. Accepted March 9, 1988. Financial support by FONDECYT (Chile) is duly acknowledged.

Equilibrium-Phase Properties of the Neopentane–Carbon Dioxide Binary System

Ah-Dong Leu and Donald B. Robinson*

Department of Chemical Engineering, University of Alberta, Edmonton, Alberta, Canada T6G 2G6

Vapor and liquid equilibrium-phase compositions were determined for the neopentane–carbon dioxide system at 40, 65, 90, 120, and 150 °C from the vapor pressure of neopentane to pressures in the critical region. The equilibrium ratios for each component were calculated at each temperature from the phase composition data. The critical pressure corresponding to each of the experimental temperatures was measured and the critical locus for the binary was constructed.

Introduction

Carbon dioxide is a very important industrial raw material and its uses range from the enhanced recovery of conventional and heavy oil to supercritical extraction processes in the food industry. Because of the current interest in the behavior of gas and liquid systems containing carbon dioxide, users of basic thermodynamic data are becoming increasingly sensitive to the reliability of existing data, and they show considerable interest in expanding the pressure and temperature ranges and the number of systems for which data are available.

A literature survey pertaining to the phase behavior of carbon dioxide–paraffin hydrocarbon binaries has revealed that the work of Schwartz et al. (*1*) and Stead et al. (*2*) represents the only data on the neopentane–carbon dioxide system. In their studies, the highest temperature was 27 °C. Accordingly, it was decided to carry out an experimental study of this system in the temperature range from 40 °C to near the critical temperature of neopentane. Data in this region are useful for developing improved generalized equation of state parameters for neopentane–carbon dioxide mixtures.

In addition to the phase composition measurements, critical temperatures and corresponding critical pressures were ob-

---

* Author to whom all correspondence should be addressed.

0021-9568/88/1733-0313$01.50/0